Energy 43 (2012) 329–333

Contents lists available at SciVerse ScienceDirect

Energy

journal homepage: www.elsevier.com/locate/energy

# Gasification of biomass micron fuel with oxygen-enriched air: Thermogravimetric analysis and gasification in a cyclone furnace

Gong Cheng, Pi-wen He, Bo Xiao*, Zhi-quan Hu, Shi-ming Liu, Le-guan Zhang, Lei Cai

*School of Environmental Science and Engineering, Huazhong University of Science and Technology, Wuhan 430074, PR China*

ARTICLE INFO

*Article history:*
Received 13 June 2011
Received in revised form
22 March 2012
Accepted 6 April 2012
Available online 1 May 2012

*Keywords:*
Biomass micron fuel (BMF)
Autothermal gasification
Oxygen-enriched air
Cyclone furnace

ABSTRACT

The oxygen-enriched gasification of biomass micron fuel (BMF) was studied. Thermogravimetric analyses under different oxygen concentrations were performed to investigate the gasification behavior. The results showed that the increasing oxygen concentration enhanced the release of volatile matter and the combustion of fixed-carbon. The autothermal gasification of BMF using the oxygen-enriched air agent in a cyclone furnace was also studied. When the oxygen concentration increased from 21% to 31.4%, the gas yield increased from 72.14% to 81.41% and the lower heating value (LHV) of the produced gas increased to 6200 kJ/Nm$^3$.

© 2012 Elsevier Ltd. All rights reserved.

## 1. Introduction

Biomass was considered as a promising renewable energy and was expected to replace fossil fuels gradually [1,2]. Extensive researches on bio-energy from biomass were based on two major reasons: 1) it was renewable, and 2) biomass appeared to have much less contribution to the increase of the greenhouse gases than the fossil fuel [3]. Biomass thermochemical conversion process, including combustion, pyrolysis and gasification, was recognized as a widely applied technology for bio-energy conversion [4,5]. However, raw biomass materials were unfeasible for direct use in the commercial scale application, owing to the disadvantages of heterogeneity and lower heating value per unit volume [6]. Thus, a proper pretreatment method to improve the performance of biomass was essential.

Our team developed a kind of powdery biomass fuel with particle size of less than 250 μm, named as biomass micron fuel (BMF). Through an advanced crushing system with lower energy consumption, the particle size of biomass was reduced, and the homogeneity and bulk density were improved. It was more efficient for transportation, storage, feeding and utilization. The combustion of BMF in a lab-scale combustor had been investigated by Luo et al. [7]. The results showed that the average heating rate and peak temperature increased with the decrease of particle size. And the maximum combustion temperature of BMF could reach up to 1200 °C, with the 97% of combustion efficiency.

Cyclone furnace, a kind of autothermal gasifier, was designed to be similar to a cyclone dust catcher. In this gasifier, fast pyrolysis, partial combustion and gasification took place almost simultaneously, and the thermal energy was provided by partial combustion of biomass. Many studies had investigated the behavior of biomass gasification in the cyclone gasifier [8–10]. Sun et al. indicated that the peak temperature of air gasification of wood powder in the cyclone gasifier was about 850–1000 °C which was higher than that in fluidized bed gasifiers. Fuel particle was dispersed by gas flow, and was pyrolyzed and gasified individually. Therefore, there was no slagging in the cyclone gasifier [11].

Nevertheless, the produced gas from the air gasification was highly diluted by nitrogen, which led to a lower LHV. It was proved that gasification using the oxygen or oxygen-enriched air agent was considered to be possible for reducing the nitrogen dilution effect and increasing the reactor temperature. Campoy et al. suggested that the use of enriched air remarkably promoted the gasification efficiency and the LHV of the gas for air–steam gasification of biomass in a fluidized bed [12]. Yoon et al. compared the syngas produced from gasification of biodiesel by-product with air and oxygen. It revealed that the syngas heating value and carbon conversion using the oxygen agent was higher than using air [13]. Thus, the gasification with the oxygen-enriched air would be a promising technique to produce fuel gas of high quality.

In this study, thermogravimetric analysis (TGA) under different oxygen concentrations was carried out to examine the thermal

---

* Corresponding author. Tel./fax: +86 (0)27 87557464.
*E-mail addresses:* xiaobo1958@126.com, xiaobocg021@163.com (B. Xiao).

0360-5442/$ – see front matter © 2012 Elsevier Ltd. All rights reserved.
doi:10.1016/j.energy.2012.04.022

**Table 1**
Ultimate analysis and proximate analysis of the sample.

| Ultimate analysis (wt%) | | Proximate analysis (wt%) | |
|---|---|---|---|
| C | 44.54 ± 0.56 | Moisture content | 4.52 ± 0.18 |
| H | 5.36 ± 0.13 | Volatile matter | 78.46 ± 0.48 |
| O[a] | 47.78 ± 0.40 | Fixed-carbon | 15.17 ± 0.54 |
| N | 0.41 ± 0.09 | Ash | 1.85 ± 0.39 |
| S | 0.06 ± 0.008 | Higher heating value (MJ/kg) | 16.62 ± 0.32 |

[a] By difference.

kinetics of BMF. Furthermore, the performance of fuel gas produced from BMF gasification in a cyclone furnace using an oxygen-enriched air agent was investigated.

## 2. Theory and calculation

The kinetic parameters, activation energy and pre-exponential factor, are determined by the integral method [14,15]. It is assumed that solid fuel thermal decomposition is a first-order reaction.

The results of thermogravimetric experiments are expressed as a function of conversion $X$, which is defined as

$$X = (W_0 - W_t)/\left(W_0 - W_f\right) \tag{1}$$

where $W_0$ is the initial mass of sample; $W_t$ is the mass of pyrolyzed sample and $W_f$ is the final residual mass.

The BMF gasification reaction equation may simply be expressed as the following formula:

$$\mathrm{d}X/\mathrm{d}t = A\exp(-E/RT)(1-X) \tag{2}$$

The above rate expression can be transformed into non-isothermal rate expressions describing reaction rates as a function of temperature at a constant $\beta$ ($\beta = \mathrm{d}T/\mathrm{d}t$):

$$\mathrm{d}X/\mathrm{d}T = A/\beta\cdot\exp(-E/RT)(1-X) \tag{3}$$

Integrating up to conversion ($X$) and substituting the temperature integral and taking the logarithm,

$$\ln\left[-\ln(1-X)/T^2\right] = \ln(AR/\beta E) - E/RT \tag{4}$$

In Eqs. (2)–(4), $A$ and $E$ are the Arrhenius parameters, pre-exponential factor and activation energy, respectively; $\beta$ is the heating rate.

For each conversion value, $\ln[-\ln(1-X)/T^2]$ plotted versus $1/T$ may give a straight line if the process can be assumed as a first-order reaction. From the slope and the intercept, the activation energy $E$ and the pre-exponential factor $A$ can be determined, respectively.

## 3. Materials and methods

### 3.1. Materials

The selected BMF was produced from ramie residues collected in Xianning City, Hubei Province, China. The samples were dried under the sun for a period of 7 days to reduce the moisture content and then were shredded into particles of sizes between 80 and 120 μm. The proximate and ultimate analyses of the sample were listed in Table 1. Ultimate analysis of the sample was obtained with a CHNS/O analyzer (Vario Micro cube, Elementar). Such analysis gives the weight percent of carbon, hydrogen, nitrogen, and sulfur in the sample simultaneously, and the weight percent of oxygen is determined by difference. The thermogravimetric analyzer was used to carry out the proximate analysis which was expressed in terms of moisture, volatile matter, fixed-carbon and ash [16].

### 3.2. Thermogravimetric analysis

Thermogravimetric analysis of the BMF sample was carried out by TA Instruments system (Diamond TG/DTA, PerkinElmer Instruments). A sample mass of 3.5 ± 0.1 mg was used for the thermogravimetric analysis in each experiment. Several different atmospheres ($N_2$:$O_2$ = 4:1, $N_2$:$O_2$ = 3:2, $N_2$:$O_2$ = 2:3, $N_2$:$O_2$ = 1:4) were performed. The heating rate was controlled at 10 °C/min from 25 °C to 800 °C.

### 3.3. Apparatus and procedures

The equipment included cyclone furnace, screw feeder, air compressor, oxygen generator, flowmeter, gas sampling, and thermocouple (K-type). The schematic configuration was illustrated in Fig. 1. The cyclone furnace (high 600 mm, outer diameter 300 mm) was made of heat-resistant stainless steel tubing with a 5 mm of wall thickness and wrapped with insulation materials.

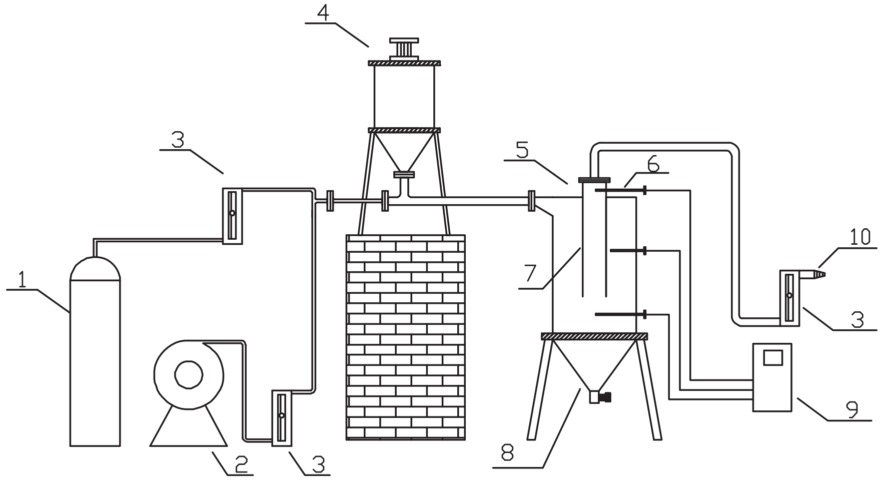

**Fig. 1.** Experimental apparatus 1, Oxygen generator; 2, Air compressor; 3, Flow meters; 4, Screw feeder; 5, Cyclone furnace; 6, Thermocouples; 7, Gas flow pipe; 8, Taper slag container; 9, Temperature measurement system; 10, Gas sampling port.

At the beginning of each experimental run, BMF was added into the hopper; the air compressor was turned on to provide an excessive air (50 $m^3$/h) at first. The screw feeder was turned on at the desired rotate speed to keep a 12 kg/h of feedstock flow rate, and then oxy-acetylene flame was used to ignite BMF in the cyclone furnace. The furnace was rapidly heated up to approximately 800 °C within 5 min. Holding the constant of ER (0.37), the air flow and the oxygen flow were simultaneously adjusted to obtain the different oxygen concentrations of 21, 22.5, 25, 28.1 and 31.4%. When the temperature in the cyclone furnace kept a stable state for 3 min, the tests began and experimental data were recorded. Because of the energy supplied by partial combustion, the temperature in the reactor might have the difference of 10–30 °C among parallel tests.

The product gas was analyzed by GC 9800 T. Permanent gases ($H_2$, $CH_4$, $N_2$, CO and $CO_2$) were analyzed with TCD using TDX-01 columns. The temperatures of injector, oven and detector were at 200, 85 and 90 °C, respectively. The carrier gas was argon in all analyses. The gas standards were mixtures of $H_2$, $CH_4$, CO and $CO_2$. With further dilutions by different volumes of pure $N_2$ standard, different concentrations of each gas compound were obtained to generate a calibration curve.

### 3.4. Methods of data processing

The lower heating value (LHV) of the product gas is calculated by [17,18],

$$\mathrm{LHV}\left(\mathrm{kJ/Nm^3}\right) = (\mathrm{CO} \times 126.36 + \mathrm{H_2} \times 107.98 + \mathrm{CH_4} \times 358.18) \tag{5}$$

Gasification efficiency, defined as the ratio of the LHV the produced gas to combustion heat of the biomass, was calculated by [19],

$$E_{\mathrm{gas}}(\%) = \mathrm{LHV_{gas}}/\mathrm{LHV_{BMF}} \times \mathrm{Y} \times 100\% \tag{6}$$

The carbon conversion efficiency is calculated by,

$$X_{\mathrm{C}}(\%) = [12Y(\mathrm{CO}\% + \mathrm{CO_2}\% + \mathrm{CH_4}\%)/22.4 \times \mathrm{C}\%] \times 100\% \tag{7}$$

where, CO, $H_2$ and $CH_4$ are the molar concentrations of components of the product gas. $Y$ is the product gas yield ($\mathrm{Nm^3/kg}$). $\mathrm{LHV_{gas}}$ is the lower heating value ($\mathrm{MJ/Nm^3}$) of the product gas, and $\mathrm{LHV_{BMF}}$ is the lower heating value (MJ/kg) of the BMF feedstock. C% is the mass percentage of carbon in ultimate analysis of the sample.

## 4. Results and discussion

### 4.1. Thermogravimetric analysis

#### 4.1.1. Effect of oxygen concentration

The typical TGA plots of BMF under different oxygen concentrations are shown in Fig. 2. It can be seen that three stages are determined according to the approximate starting and end points of the DTG curves. The first stage of weight loss ranged from 25 °C to 120 °C, in which a relative small change of sample mass was attributed to the loss of water and light volatile compounds in the sample. Following the first stage, there was negligible weight loss (about 0.5%) in the temperature range of 120–250 °C. The major mass loss step occurred between 250 °C and 490 °C, and the DTG curve showed two observable peaks in this region. This suggested that this region could be divided into two stages corresponded to different thermochemical reactions. The temperature from 250 °C to 390 °C was regarded as the second stage, in which the main weight loss was due to removal of the volatile matters of the sample. In the third stage (ranged from 390 °C to 490 °C), about 20% of weight loss was due to oxidation of the char remaining after the volatiles were removed from the sample.

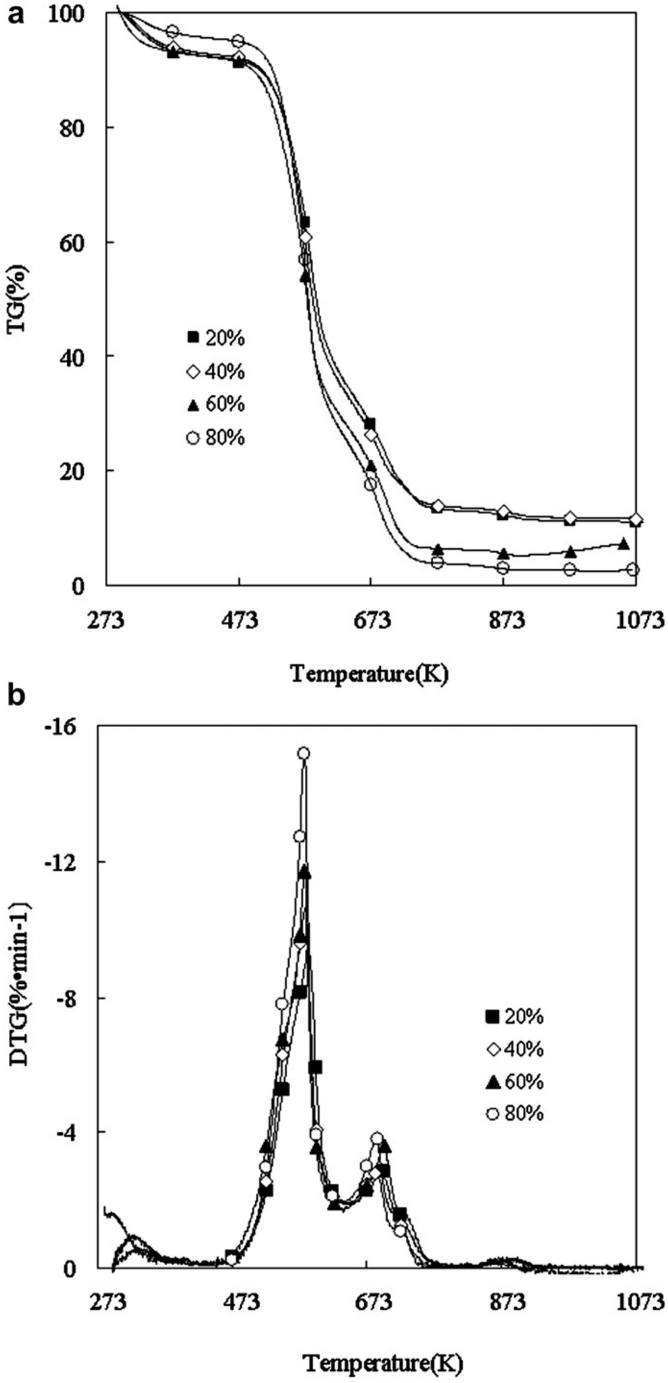

**Fig. 2.** TG and DTG curves under different oxygen concentrations.

When oxygen concentration increased from 20% to 80%, the maximum weight loss rate in the second stage regularly increased from 9.47%/min to 15.15%/min and the peak temperature varied from 313 °C to 306 °C. This indicated that volatiles in the sample released more quickly and shorter time was consumed to reach the peak temperature under higher oxygen concentration. In the char combustion stage, the weight loss rate slightly increased and peak temperature also shifted to a lower temperature with the increasing oxygen concentration. Similar results were observed by Fang et al. [20] during the pyrolysis and coke combustion processes of cotton straw and merbau under different oxygen concentrations. However, the effect of oxygen concentration on the thermogravimetric characteristic of various materials was quite different. Liu et al. [21] studied the oxygen-enriched air combustion of paper mill sludge, which consisted of 59.30% of moisture, 5.06% of volatile matter, 16.95% of fixed-carbon and 18.69% of ash. The maximum weight loss rate regularly increased in the volatile releasing stage, while it declined in the char combustion stage when oxygen concentration was below 40%.

### 4.1.2. Kinetic parameters

The data in the second stage and the third stage were respectively used for determining kinetic parameters. The obtained results are listed in Table 2. It is clear that the regression coefficients ($r$) are almost greater than 0.99. The calculated activation energy in the second stage ranged from 55.52 kJ/mol to 72.72 kJ/mol, and the value in the third stage was from 23.90 kJ/mol to 29.04 kJ/mol. It can be seen that the activation energy decreases along with the pyrolysis process and char combustion process for all the runs. Mansaray et al. reported the similar results, and they suggested that lignin condensed to char had lower decomposition rates than cellulose and hemicellulose components [22].

During the processes of pyrolysis and combustion, the activation energy of cellulosic materials was affected by several factors such as decrease of activated molecule concentration, diffusion limitation and organic impurities [20]. In this study, the values both in the two stages regularly increased with the increasing oxygen concentration. Similar results on the combustion of rice and wheat straw were observed by Yu et al. [23], whose conclusion showed that the activation energy of combustion with or without catalyst in the oxygen-enriched atmosphere was usually higher than that in air atmosphere.

## 4.2. Oxygen-enriched gasification in a cyclone furnace

In the present work, the autothermal gasification of BMF with oxygen-enriched air in the cyclone furnace was studied. The reactor temperature was measured at different points of the furnace and the mean value was recorded in this test. The temperatures reached 798, 803, 820, 838 and 845 °C at oxygen concentrations of 21, 22.5, 25, 28.1 and 31.4%, respectively. At a constant of ER, the increase in oxygen concentration meant that the decreasing nitrogen flow had to be heated. Thus, the increase in reactor temperature may result from the decreasing heat loss.

### 4.2.1. Products distribution

The products (gas, tar and char) distribution from the BMF gasification under different oxygen concentrations was given in Fig. 3. With the increasing oxygen concentration, the yields of tar and char respectively decreased from 12.17% to 3.75% and from 15.69% to 14.84%, while the gas yield gradually increased from 72.14% to 81.41%. The further tar decomposition and char combustion contributed to the increase in gas yield. The variation was attributed to the increasing reactor temperature under the higher oxygen concentration. The greater temperatures favored the production of gas. In addition, the increasing oxygen concentration led to the increasing rates of volatile matter release and of char combustion (From Fig. 2). Thus, the sample was easier to be converted into the gas product under the higher oxygen concentration.

**Table 2**
Kinetic parameters under different oxygen concentrations.

| Oxygen concentration (%) | | 20 | 40 | 60 | 80 |
|---|---|---|---|---|---|
| Second stage | $E$ | 55.52 | 55.72 | 59.92 | 72.72 |
| | $A$ | $2.43 \times 10^5$ | 10.98 | 37.05 | 17.08 |
| | $r$ | 0.9845 | 0.9970 | 0.9982 | 0.9955 |
| Third stage | $E$ | 24.18 | 24.53 | 27.87 | 29.04 |
| | $A$ | $3.48 \times 10^2$ | $5.84 \times 10^{-3}$ | $1.14 \times 10^{-2}$ | $1.14 \times 10^{-2}$ |
| | $r$ | 0.9619 | 0.9858 | 0.9888 | 0.9557 |

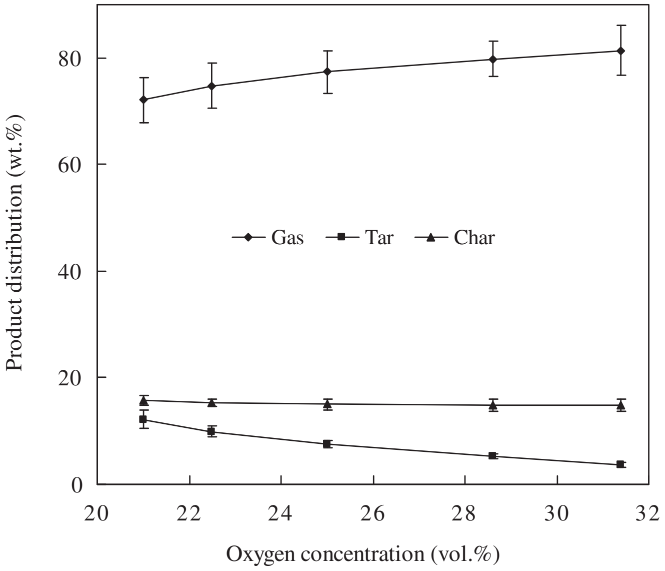

**Fig. 3.** Effect of oxygen concentration on product distribution.

### 4.2.2. Gas composition

Fig. 4 depicts the effect of oxygen concentration in oxygen-enriched air on the gas composition. The volume fractions of the main gas species (H2, CO, CO2 and CH4) were measured. It can be seen that the compositions of produced gases including H2, CO, CO2 and CH4 generally increases at different levels due to the decrease in the nitrogen dilution. When the oxygen increased from 21% to 31.4%, a sharp increase in CO2 concentration was observed. Also, the concentrations of H2 and CO respectively increased from 8.83% to 12.01% and from 18.08% to 23.93%. It was noted that CH4 concentration slowly increased from 2.96% to 4.66% with the

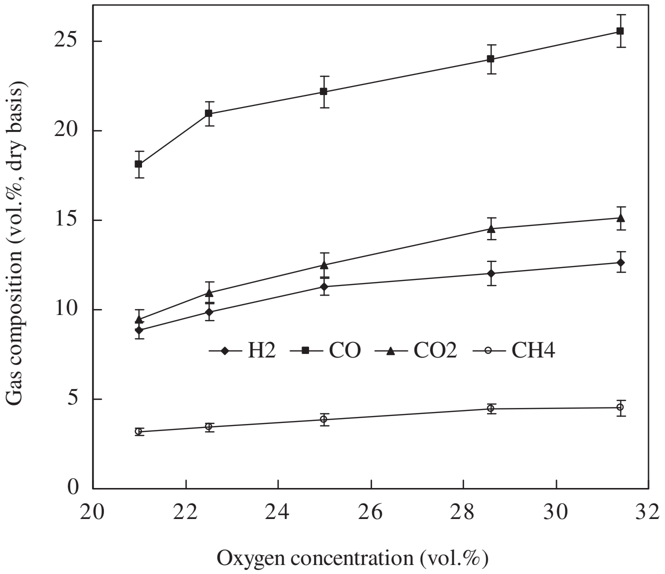

**Fig. 4.** Effect of oxygen concentration on gas composition.

**Table 3**
Gasification performance of BMF with the oxygen-enriched air.

| Oxygen concentration (vol.%) | 21 | 22.5 | 25 | 28.6 | 31.4 |
|---|---|---|---|---|---|
| LHV (kJ/Nm$^3$) | 4377 ± 215 | 4930 ± 256 | 5391 ± 263 | 5915 ± 201 | 6200 ± 292 |
| Carbon conversion efficiency (%) | 61.00 ± 1.13 | 64.00 ± 1.74 | 67.81 ± 2.05 | 70.86 ± 2.23 | 71.76 ± 1.96 |
| Gasification efficiency (%) | 52.14 ± 1.04 | 53.75 ± 0.96 | 57.06 ± 0.47 | 58.64 ± 0.46 | 60.03 ± 0.85 |

increasing oxygen concentration. It was quite different from the result obtained from biomassndashoxygen gasification in a high-temperature entrained-flow gasifier [24]. In their study, the CH4 content in produced gas was negligible and a decrease trend appeared with the increasing oxygen/biomass ratio.

### 4.2.3. Gasification performance

The gasification performance of BMF with the oxygen-enriched air in the cyclone furnace was shown in Table 3. As expected, the LHV of the product gas remarkably increased from 4377 kJ/Nm$^3$ to 6200 kJ/Nm$^3$ when the oxygen concentration varied from 22.5% to 31.4%. It can be explained by the significant increase in the combustible gas ($H_2$, CO and $CH_4$). Generally, the LHV of produced gas from air gasification of cellulosic biomass was about 3000–5000 kJ/Nm$^3$ for fixed bed gasifier [25] and many kinds of autothermal gasifiers [24]. In a clapboard-type internal circulating fluidized bed gasifier, rice husk gasification gas had a maximum heating value of around 5000 kJ/Nm$^3$ [24]. And the value of the gas from rice husk gasification in an entrained-flow reactor was between 3.08 MJ/Nm$^3$ to 4.74 MJ/Nm$^3$ when the reactor temperature was 800 °C [26]. The research on air gasification of BMF in the cyclone furnace showed that the LHV of the gas was about 4000 kJ/Nm$^3$ [10]. In this study, the LHV of produced gas increased by 25–40% using the oxygen-enriched air agent. Hence, the introduction of oxygen-enriched air significantly improved the quality of the fuel gas.

Furthermore, both carbon conversion efficiency and gasification efficiency slightly increased with the increasing oxygen concentration. The change could be interpreted by the fact that more tar was converted to the fuel gas under the higher oxygen concentration.

## 5. Conclusions

Thermogravimetric analysis showed that both the volatile release rate and the fixed-carbon combustion rate increased with the increasing oxygen concentration. In the cyclone furnace, the gasification of BMF with oxygen-enriched air was affected by oxygen concentration. When the oxygen concentration increased from 21% to 31.4%, the gas yield increased from 72.14% to 81.41%, carbon conversion efficiency increased from 61.00% to 71.76%, and gasification efficiency increased from 52.14% to 60.03%. Under the operating conditions, the maximum LHV of the produced gas reached 6200 kJ/Nm$^3$. The gasification of BMF using the oxygen-enriched air agent significantly improved the quality of the fuel gas.

## Acknowledgements

This research was supported by the National Natural Science Foundation of China (No. 20876066). The authors are grateful to the Analytical and Testing Center of Huazhong University of Science and Technology for carrying out the ultimate analysis and the thermogravimetric analysis of the samples.

## References

[1] Karamarkovic R, Karamarkovic V. Energy and exergy analysis of biomass gasification at different temperatures. Energy 2010;35:537–49.

[2] Prins MJ, Ptasinski KJ, Janssen FJJG. More efficient biomass gasification via torrefaction. Energy 2006;31:3458–70.

[3] Cao Y, Wang Y, Riley JT, Pan WP. A novel biomass air gasification process for producing tar-free higher heating value fuel gas. Fuel Process Technol 2006; 87:343–53.

[4] Dare P, Gifford J, Hooper RJ, Clemens AH, Damiano LF, Gong D, et al. Combustion performance of biomass residue and purpose grown species. Biomass Bioenergy 2001;21:277–87.

[5] Xiao RR, Chen XL, Wang FC, Yu GS. Pyrolysis pretreatment of biomass for entrained–flow gasification. Appl Energy 2010;87:149–55.

[6] Ndiema CKW, Manga PN, Ruttoh CR. Influence of die pressure on relaxation characteristics of briquetted biomass. Energy Convers Manage 2002;43: 2157–61.

[7] Luo SY, Xiao B, Hu ZQ, Liu SM, He MY. Experimental study on combustion of biomass micron fuel (BMF) in cyclone furnace. Energy Convers Manage 2010; 51:2098–102.

[8] Gabra M, Pettersson E, Backman R, Kjellström B. Evaluation of cyclone gasifier performance for gasification of sugar cane residue-Part 1: gasification of bagasse. Biomass Bioenergy 2001;21:351–69.

[9] Gabra M, Pettersson E, Backman R, Kjellström B. Evaluation of cyclone gasifier performance for gasification of sugar cane residue-Part 2: gasification of cane trash. Biomass Bioenergy 2001;21:371–80.

[10] Guo XJ, Xiao B, Liu SM, Hu ZQ, Luo SY, He MY. An experimental study on air gasification of biomass micron fuel (BMF) in a cyclone gasifier. Int J Hydrogen Energy 2009;34:1265–9.

[11] Sun SZ, Zhao YJ, Tian HM, Ling F, Su FM. Experimental study on cyclone air gasification of wood powder. Bioresour Technol 2009;100:4047–9.

[12] Campoy M, Gómez-Barea A, Vidal FB, Ollero P. Air–steam gasification of biomass in a fluidized bed: process optimisation by enriched air. Fuel Process Technol 2009;90:677–85.

[13] Yoon SJ, Choi YC, Son YI, Lee SH, Lee JG. Gasification of biodiesel by-product with air or oxygen to make syngas. Bioresour Technol 2010;101:1227–32.

[14] Yorulmaz SY, Atimtay AT. Investigation of combustion kinetics of treated and untreated waste wood samples with thermogravimetric analysis. Fuel Process Technol 2009;90:939–46.

[15] Otero M, Sanchez ME, Gómez X, Morán A. Thermogravimetric analysis of biowastes during combustion. Waste Manage 2010;30:1183–7.

[16] Lua AC, Guo J. Preparation and characterization of chars from oil palm waste. Carbon 1998;36:1663–70.

[17] Lv PM, Xiong ZH, Chang J, Wu CZ, Chen Y, Zhu JX. An experimental study on biomass air–steam gasification in a fluidized bed. Bioresour Technol 2004;95:95–101.

[18] Mun TY, Seon PG, Kim JS. Production of a producer gas from woody waste via air gasification using activated carbon and a two-stage gasifier and characterization of tar. Fuel 2010;89:3226–34.

[19] He MY, Xiao B, Liu SM, Guo XJ, Luo SY, Xu ZL, et al. Hydrogen-rich gas from catalytic steam gasification of municipal solid waste (MSW): influence of steam to MSW ratios and weight hourly space velocity on gas production and composition. Int J Hydrogen Energy 2009;34:2174–83.

[20] Fang MX, Shen DK, Li YX, Yu CJ, Luo ZY, Cen KF. Kinetic study on pyrolysis and combustion of wood under different oxygen concentrations by using TG-FTIR analysis. J Anal Appl Pyrol 2006;77:22–7.

[21] Liu K, Ma XQ, Xiao HM. Experimental and kinetic modeling of oxygen-enriched air combustion of paper mill sludge. Waste Manage 2010;30:1206–11.

[22] Mansaray KG, Ghaly AE. Determination of kinetic parameters of rice husks in oxygen using thermogravimetric analysis. Biomass Bioenergy 1999;17:19–31.

[23] Yu ZS, Ma XQ, Liu A. Kinetic studies on catalytic combustion of rice and wheat straw under air- and oxygen-enriched atmospheres, by using thermogravimetric analysis. Biomass Bioenergy 2008;32:1046–55.

[24] Zhou ZQ, Ma LL, Yin XL, Wu CZ, Huang LC, Wang C. Study on biomass circulation and gasification performance in a clapboard-type internal circulating fluidized bed gasifier. Biotechnol Adv 2009;27:612–5.

[25] Plis P, Wilk RK. Theoretical and experimental investigation of biomass gasification process. Energy 2011;36:3838–45.

[26] Zhao YJ, Sun SZ, Tian HM, Qian J, Su FM, Ling F. Characteristics of rice husk gasification in an entrained flow reactor. Bioresour Technol 2009;100:6040–4.